

A Novel Up-Link Code-Acquisition Procedure based on a Structured Preamble Sequence

Marco Villanti, Paola Salmi, Raffaella Pedone, and Giovanni Emanuele Corazza

DEIS/ARCES - University of Bologna

Viale Risorgimento, 2 - 40136 - Bologna - Italy

email: {mvillanti,psalmi,rpedone,gecorazza}@deis.unibo.it

Abstract— In this paper, a novel up-link one-shot code acquisition procedure is proposed based on a structured preamble sequence. The general strategy is applied to the context of third generation satellite networks. A multi-dwell approach is introduced to simplify the detection of a long preamble. The parallel detection of the two basic sequences constituting the preamble is coordinated by a novel HLC (High Level Controller). Active and passive differential post detection integrations are selected to perform detection during the search and verification phases, respectively. Performance is evaluated and optimized with respect to system parameters.

I. INTRODUCTION

The sharply increasing demand for new communication services, in particular for multimedia data applications, is pushing the interests and efforts of the scientific community toward the deployment of 3G (3rd Generation) systems, along with the development of 4G (4th Generation) evolutions. In this framework, the efficient provision of DMB (Digital Multimedia Broadcasting) services represents a mandatory objective to be achieved in the medium term. The optimal air interface to support DMB services should build upon standard point-to-point radio access formats, such as W-CDMA (Wideband-Code Division Multiple Access), and introduce the necessary ameliorations and hooks to effectively support point to multi-point connections. A satellite based overlay network seems to be one of the most efficient approaches to solve this technical challenge. In fact, besides being able to cover vast regions, the satellite is a more effective medium for broadcasting information to subsets/groups of users, or even to the entire population. In this way, the integration between terrestrial and satellite networks overcomes the classic geographic complementar-

ity concept, which by the way has proved to be quite unattractive in terms of building a strong business case for a mass-market satellite system. Rather, intertwined service integration is pursued to produce an undebatable business opportunity for entering the horizontal market, finally freeing the satcom world from the cage of niche markets. This idea of integration among heterogeneous networks has been taken up by the European IST funded project SATIN [2] and its sequel MODIS and MAESTRO [1] that has proposed a system architecture envisaging both the terrestrial and satellite networks. In particular, the main goal of this project is the evaluation of the feasibility of the DMB services delivery, and its impact on the radio interface design.

The S-UMTS (Satellite - Universal Mobile Telecommunications System) air interface, i.e. the SW-CDMA (Satellite W-CDMA) standard, proposed by ETSI (European Telecommunications Standards Institute), has been adapted to the SATIN system architecture, introducing the required modifications to achieve an effective network integration. In particular, the SATIN project foresees two different options for the return link: a direct return link through the satellite network and a return link through the terrestrial network. An asynchronous return-link channel, i.e. the RACH (Random Access CHannel), is foreseen to achieve the first connection among mobile terminals and base stations, and to send short data packets. The preamble detection over this asynchronous channel has been studied in this work introducing a novel procedure to perform code acquisition, that results to be one of the most critical issues in the W-CDMA air interface. Even if this approach has been applied to S-UMTS third

generation systems, it can be more generally employed in many different applications, where a long preamble is required.

The novelty of the paper is mainly related to the exploitation of a structured preamble, composed by a series of equal subsequences terminated by a unique word. This allows to introduce a multi-dwell strategy for up-link code acquisition, that foresees the employment of two parallel sequence detectors controlled by a new ad-hoc architecture. The proposed strategy turns out to be very flexible and general, being robust against a given number of missed detection events, and including the immediate rejection option as a special case. Dealing with an uplink packet transmission, the multi-dwell procedure is completed in single preamble processing, therefore the acquisition process results to be one-shot and performance must be evaluated in terms of *preamble missed detection* and *preamble false alarm* probability. Performance has been evaluated and optimized through simulations as a function of detection thresholds and number of allowed missed detections.

II. SYSTEM MODEL

Uplink code acquisition, namely signature detection and code epoch estimation, is performed exploiting a known preamble. A terrestrial-like approach, where the message part is sent only after the preamble acquisition acknowledgement, is too costly in a satellite environment, due to the presence of a large propagation delay. For this reason, preamble and message part joint transmission has been preferred, and an asynchronous access scheme has been selected in [3], [4]. In particular, the preamble consists of 8 repetitions of the same word identified as C_{pre} , followed by the unique word, namely C_{UW} , that marks the end of the preamble. The corresponding preamble structure is depicted in fig. 1. The C_{pre} is a 4096 chip-long complex sequence obtained by multiplying the base station scrambling code for 256 repetitions of a signature chosen from the OVSF (Orthogonal Variable Spreading Factor) code tree of length 16. Notably, the C_{pre} is equal to the preamble adopted in the terrestrial UMTS standard, so allowing the compatibility between the terrestrial and satellite networks. The C_{UW} is obtained by multiplying the C_{pre} for a known QPSK modu-

lated sequence.

The detection of the whole sequence through a typical matched filter approach seems to be not practicable on actual systems because of the resulting detector complexity. The modular preamble structure suggests to perform acquisition by splitting the entire sequence detection into the detection of two shorter sequences, aiming at an overall complexity reduction. Accordingly, two different detectors are employed for the C_{pre} and C_{UW} , respectively. The detector design must counteract the degradation introduced by the presence of the frequency error, mainly due to the oscillators mismatch, and terminal/satellite motions. As a consequence, coherent correlation has to be performed over a $C_{\text{pre}}/C_{\text{UW}}$ subsequence, and a PDI (Post Detection Integration) has to be envisaged. Different PDI techniques could be considered, such as NCPDI (Non-Coherent PDI) [5], DPDI (Differential PDI) [6] and ML-PDI (Maximum Likelihood PDI) [7]. For satellite communications, typical values of the frequency error range from some hundreds to a few thousands of Hz, and in this case DPDI turns out to be one of the most promising PDI scheme, as discussed in [6]. The adoption of a ML-PDI scheme could provide better performance than DPDI, but an increased computational complexity would be introduced. For this reason, being interested in a low complexity acquisition procedure, DPDI seems to be the natural choice to be adopted for both C_{pre} and C_{UW} detection. Therefore, the detection scheme can be duplicated using two different sequence generators.

Each detector is characterized by the performance in terms of false alarm probability, P_{fa}^P and P_{fa}^U , and missed detection probability, P_{md}^P and P_{md}^U , for the C_{pre} and C_{UW} , respectively. In the following, the notation $\hat{H}_1(C_{\text{UW}})$ identifies the event that the decision variable exceeds the threshold: this case determines a false alarm or a missed detection, under the hypotheses $H_0(C_{\text{UW}})$, C_{UW} absence, and $H_1(C_{\text{UW}})$, C_{UW} presence, respectively. A similar notation is adopted for C_{pre} .

Both active and passive realization of the DPDI detector are employed as specified in section III. The associated block diagrams are reported in figs. 2-3, respectively, where ξ is the generic decision threshold, M is the coherent integration length,

and L indicates the PDI duration.

III. HIGH LEVEL CONTROLLER

The outputs of the C_{pre} and C_{UW} detectors are opportunely processed to achieve the entire preamble acquisition according to a two-step procedure. The related functional block diagram is shown in fig.4. The first step foresees an initial C_{pre} acquisition (search phase), while the second step (verification phase) involves the acquisition of the rest of the preamble according to a multi-dwell strategy controlled by the HLC (High Level Controller). In the initial step, the detector complexity is the same as a single DPDI scheme. The passive realization, is adopted in order to limit the delay. Instead, during the second step two active detectors are used at the same time in order to detect C_{pre} and C_{UW} in a parallel manner. In fact, since only a single epoch and signature hypothesis has to be verified in this phase, the active realization limits complexity and power consumption. As a consequence, considering the two-step procedure as a whole, the overall complexity decreases with respect to a filter matched to the entire preamble, as suggested by a Bayesian detector. The apparent performance worsening due to the shorter accumulation (with respect to the entire preamble length) can be limited if a smart HLC algorithm is designed. Performance of the entire preamble acquisition procedure is evaluated in terms of *preamble* false alarm probability, P_{fa} , and *preamble* missed detection probability, P_{md} , that are functions of C_{pre} and C_{UW} detector performance, $P_{fa}^{P/U}$, $P_{md}^{P/U}$.

For multi-dwell acquisition procedures, two different rejecting strategies can be in general adopted, depending on the number of tolerated missed detections, \hat{N}_{MD} , during the verification phase:

- *immediate rejection*, i.e. the procedure is stopped as soon as a missed detection occurs ($\hat{N}_{MD} = 0$);
- *no-immediate rejection*, i.e. the procedure continues until \hat{N}_{MD} missed detections have occurred.

The former solution aims at reducing the false alarm probability, while the latter at limiting the missed detection probability, so facing possible temporary fading notches. In this work, the more general case of no-immediate rejection is investigated, and immediate rejection can be obtained as

a particular case.

The HLC is designed to work in accordance with the flow-chart reported in fig. 5, where PW indicates the index of the next preamble word to be processed, and MD is a counter of the occurred missed detections. The employed preamble structure allows to assign different relevance to the events $\hat{H}_1(C_{\text{pre}})$ and $\hat{H}_1(C_{\text{UW}})$. In particular, the acquisition procedure can terminate in two different states:

- (a) *Preamble Termination Identified (PTI)*, that is reached if the C_{UW} is detected during the verification phase, corresponding to the occurrence of the event $\hat{H}_1(C_{\text{UW}})$;
- (b) *Max Dwells Performed (MDP)*, that is reached when 8 C_{pre} and one C_{UW} have been processed, but the C_{UW} has not been detected.

Under the hypothesis of preamble absence, H_0 , a preamble false alarm can occur in two different cases:

1. a C_{pre} false alarm occurs during the search and, optionally, verification phase, and a C_{UW} false alarm occurs during verification phase, i.e. the algorithm ends in the PTI state;
2. a number of $(8 - \hat{N}_{MD})$ C_{pre} false alarms over 8 processed words occurs, and the C_{UW} is correctly rejected, i.e. the algorithm ends in the MDP state discussed above.

Furthermore, under the hypothesis of preamble presence, H_1 , a preamble false alarm can occur when several C_{pre} are correctly acquired whilst a C_{UW} false alarm occurs, determining the interruption of the acquisition procedure at an incorrect instant.

It can be noted that the probability of the MDP state under H_0 is extremely low. Differently, considering the hypothesis of preamble presence, H_1 , the event of missing C_{UW} during the verification phase can occur more frequently, i.e. P_{md}^U is not in general negligible. For this reason, in this work the preamble has been considered acquired even when the procedure ends in the MDP state. Note that, this state can be achieved only if the first C_{pre} is detected. Moreover, it is worth noting that C_{UW} false alarms are critical events causing preamble false alarms. All these considerations must drive the choice of the detector operating thresholds.

Therefore, the complete design of the acquisition sub-system requires the setting of the relevant parameters as the detectors thresholds, $\xi_{C_{\text{pre}}}$ and

$\xi_{C_{UW}}$, and the number of admitted missed detections, \hat{N}_{MD} . In particular, according to the discussed considerations, the overall performance is improved if both P_{fa}^U and P_{md}^P are minimized, that is achieved by choosing a large $\xi_{C_{UW}}$, and a low $\xi_{C_{pre}}$ value. To counteract the performance degradation induced by the resulting large P_{fa}^P , an appropriately low value of \hat{N}_{MD} must be selected.

This criterion for parameter dimensioning, and, more in general, the consistency of the introduced design choices, have been validated through numerical results, as shown in section IV.

IV. PERFORMANCE EVALUATION

Performance evaluation for the proposed HLC scheme has been obtained through simulations in AWGN channel, with a signal to noise ratio equal to $E_c/N_0 = -21$ dB, where E_c identifies the average chip energy, and N_0 is the one-sided noise power spectral density. The detector parameters have been set to $M = 256$ and $L = 16$, so that $M \cdot L = 4096$, i.e. the entire preamble length. Performance in terms of P_{fa} and P_{md} is shown.

In figs. 6 - 9, preamble false alarm and missed detection probabilities, P_{fa} and P_{md} , are reported as a function of the C_{UW} threshold, $\xi_{C_{UW}}$, with the C_{pre} threshold, $\xi_{C_{pre}}$, as a parameter. In particular, $\xi_{C_{UW}}$ varies in the range 2.0-8.0, while $\xi_{C_{pre}}$ is lower according to the design criterion introduced in the previous section, and is in the range 1.0-4.0. Each figure corresponds to a different value of \hat{N}_{MD} : $\hat{N}_{MD} = 0$, i.e. immediate rejection strategy, and $\hat{N}_{MD} = 1, 2, 3$ are considered, respectively. It can be observed that there is a value of \hat{N}_{MD} that jointly minimizes P_{fa} and P_{md} . In particular, for the considered cases, the immediate rejection strategy is not the best solution, as it yields large values of P_{md} , although low values of P_{fa} can be actually obtained. Instead, by setting $\hat{N}_{MD} = 1$ or $\hat{N}_{MD} = 2$, the tradeoff between P_{md} and P_{fa} is solved in a more advantageous way by choosing high values of $\xi_{C_{UW}}$. Finally, $\hat{N}_{MD} = 3$ yields a large P_{fa} value that is not compensated by an acceptable improvement of the detection performance.

The presented numerical results point out that P_{md} varies with $\xi_{C_{UW}}$ value, but according to an evident weak dependence. This is mainly due to the fact that, in most of the actual cases, the al-

gorithm ends in the MDP state because the low value selected for $\xi_{C_{pre}}$ allows the detection of the first C_{pre} of the preamble.

In fig. 7 the C_{UW} detector performance, P_{fa}^U and P_{md}^U is also reported in order to highlight the gain introduced by the HLC.

Finally, in fig. 10, P_{fa} and P_{md} , are reported as a function of \hat{N}_{MD} , for $\xi_{C_{UW}} = 8.0$, and for different values of $\xi_{C_{pre}}$. It can be observed that a satisfactory trade-off between P_{md} and P_{fa} can be achieved with \hat{N}_{MD} just equal to 1.

V. CONCLUSIONS

In this work, a novel multi-dwell procedure for code acquisition has been proposed for up-link satellite networks. Acquisition is achieved in two steps through a HLC that handles the two different preamble sub-words, C_{pre} and C_{UW} , detectors outputs.

Differential post detection integration technique has been employed for C_{pre} and C_{UW} detection, in the passive and active realization for the search and verification phases, respectively.

A flexible HLC algorithm has been introduced and evaluated. The proposed solution provides satisfactory performance, yielding both P_{md} and P_{fa} less than 10^{-3} for $E_c/N_0 = -21$ dB properly selecting a large value for the C_{UW} threshold, reducing at the same time the detector complexity, with respect to the typical matched filter approach.

ACKNOWLEDGEMENT

This work has been partially supported by the EC IST-SATIN project (IST 2000-25030) and MAESTRO project (IST-2003-507023).

REFERENCES

- [1] IST-2003-507023 MAESTRO - Mobile Applications & sErvices based on Satellite & Terrestrial inteRwOrking project (MAESTRO)- <http://ist-maestro.dyndns.org>
- [2] IST2000 - SATIN (SATellite Ip-based Network), Deliverable D5, "S-UMTS Packet-based Layer 1 & Layer 2 functions", 2003, <http://www.ee.surrey.ac.uk/satin/>.
- [3] ETSI TS 101 851-1 (S-UMTS-A 25.211), "Satellite Component of UMTS/IMT 2000; A-family; Part 1: Physical channels and mapping of transport channels into physical channels", version V1.1.1.
- [4] ETSI TS 101 851-4 (S-UMTS-A 25.213), "Satellite Component of UMTS/IMT 2000; A-family; Part 3: Spreading and modulation", version V1.1.1.
- [5] R. De Gaudenzi, F. Giannetti, and M. Luise, "Signal Recognition and Signature Code Acquisition in CDMA

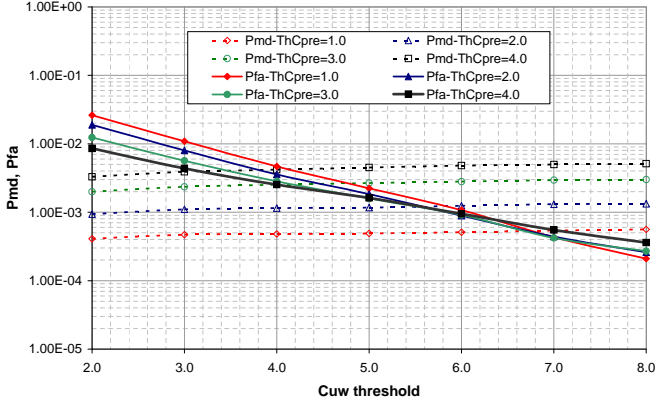


Fig. 6. HLC performance for $\hat{N}_{MD}=0$ (immediate rejection). AWGN channel, $E_c/N_0=-21$ dB

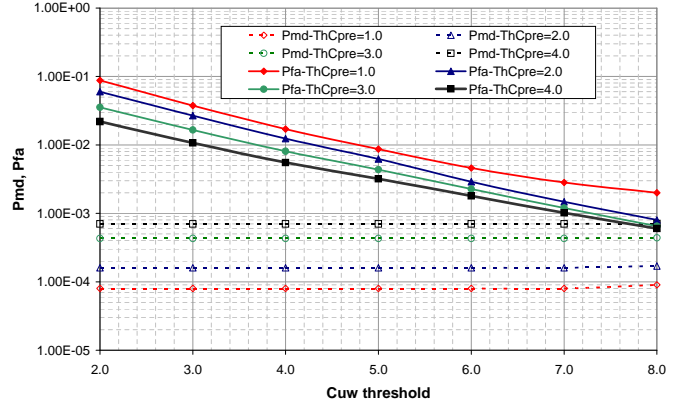


Fig. 9. HLC performance for $\hat{N}_{MD}=3$. AWGN channel, $E_c/N_0=-21$ dB

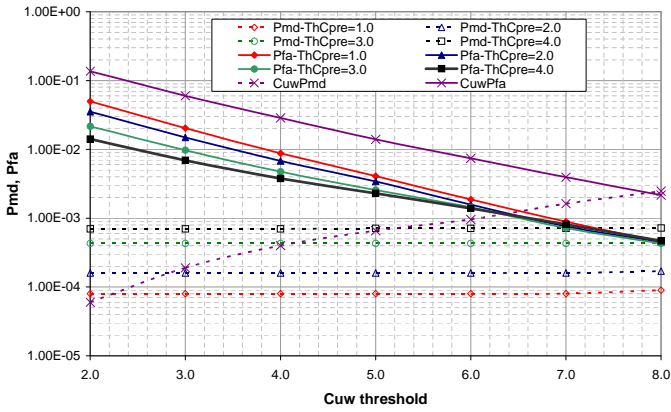


Fig. 7. HLC performance for $\hat{N}_{MD}=1$. AWGN channel, $E_c/N_0=-21$ dB. P_{md}^U and P_{fa}^U are also reported as a benchmark.

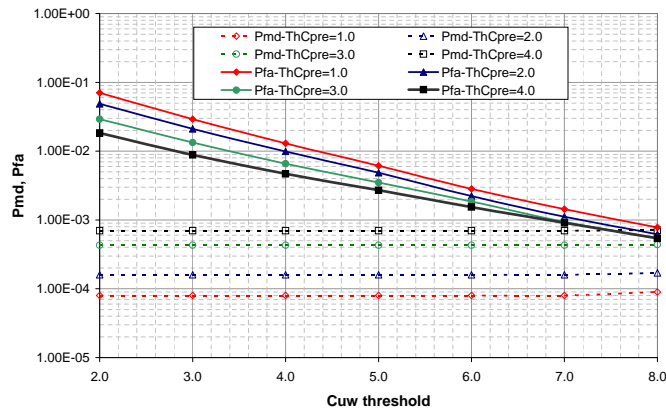


Fig. 8. HLC performance for $\hat{N}_{MD}=2$. AWGN channel, $E_c/N_0=-21$ dB

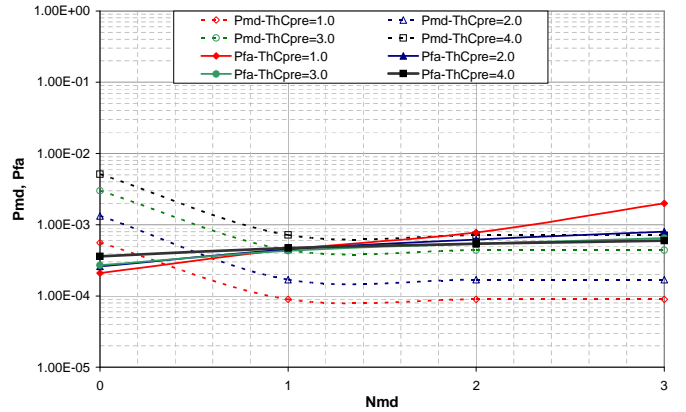


Fig. 10. HLC performance vs \hat{N}_{MD} for $\xi_{Cuw} = 8.0$. AWGN channel, $E_c/N_0=-21$ dB